Journal of Cosmology and Astroparticle Physics
An IOP and SISSA journal

Non-linear resonance in bouncing braneworld universes and initial conditions for inflation

R F Aranha[1], H P de Oliveira[2], I Damião Soares[1] and E V Tonini[3]

[1] Centro Brasileiro de Pesquisas Físicas, Rua Dr Xavier Sigaud 150, Urca, Rio de Janeiro, CEP 22290-180-RJ, Brazil
[2] Instituto de Física, Universidade do Estado do Rio de Janeiro, CEP 20550-013, Rio de Janeiro, RJ, Brazil
[3] Centro Federal de Educação Tecnológica do Espírito Santo, Avenida Vitória, 1729, Jucutuquara, Vitória CEP 29040-780-ES, Brazil
E-mail: rfaranha@cbpf.br, hahuga@gmail.com, ivano@cbpf.br and tonini@cefetes.br

Received 18 July 2007
Accepted 20 September 2007
Published 12 October 2007

Online at stacks.iop.org/JCAP/2007/i=10/a=008
doi:10.1088/1475-7516/2007/10/008

Abstract. We examine the phase space dynamics of closed Friedmann–Robertson–Walker universes with a massive inflaton field, where the Friedmann equations contain additional terms arising from high energy corrections to cosmological scenarios. The model is based upon a Randall–Sundrum type of action, with an extra timelike dimension, and the corrections implement non-singular bounces in the early evolution of the universe. In narrow windows of the parameter space of the models non-linear resonance phenomena of Kolmogorov–Arnold–Moser tori are shown to occur, leading to the destruction of tori that trap the inflaton. As a consequence the escape into inflation takes place. These resonance windows are labeled with an integer $n \geq 2$, where n is related to the ratio of the frequencies in the scale factor to those in the scalar field degrees of freedom. We examine the constraints imposed by non-linear resonance in the physical domain of parameters of the model so that inflation may be realized. The larger the order n of the resonance, the stronger the gravitational interaction in the braneworld universe inflated from initial conditions connected with the resonance considered. We also discuss the structural stability of the resonance pattern, the complex dynamics arising in this pre-inflationary phase and some of its possible imprints in the physics of inflation.

Keywords: inflation, cosmological applications of theories with extra dimensions

1475-7516/07/10008+21$30.00

JCAP10(2007)008

Contents

1. Introduction

We may consider that the initial conditions of our present expanding Universe were fixed when the early Universe emerged from the semi-classical Planckian regime and started its classical evolution. By evolving back the initial conditions using Einstein classical equations, the Universe is driven towards a singular point, where the classical regime is no longer valid. In this domain, quantum processes must be taken into account. Among several propositions a recent and quite attractive one is provided by string based formalism of D-branes that encompass general relativity as a low energy limit of a quantum gravity theory [1]. In this scenario extra dimensions are introduced, the bulk space, and all the matter in the universe would be trapped on a brane with three spatial dimensions; only gravitons would be allowed to leave the surface and move in the full bulk [2]. At low energies general relativity is recovered but at high energies significant changes are introduced in the gravitational dynamics. Our main interest here is connected to the high energy/quantum corrections that are dominant in the neighborhood of the singularity, resulting in a repulsive force that avoids the singularity and leads the universe to undergo non-singular bounces. Bouncing braneworld models were constructed by Shtanov and Sahni [3] on the basis of a Randall–Sundrum-type action with one extra dimension. The corresponding modified Friedmann's equation on the brane is expressed as

$$H^2 + \frac{k}{a^2} - \frac{\Lambda_{\rm eff}}{3} = \frac{\kappa_{\rm eff}}{3}\rho + \frac{\epsilon\kappa_5^2\rho^2}{36}, \tag{1}$$

where H is Hubble's parameter and ρ is the fluid density of the model present in the brane. The parameter κ_5 is the 5-dim (five-dimensional) Einstein constant and

$$\Lambda_{\rm eff} = \Lambda_5 + \tfrac{1}{12}\kappa_5^2\epsilon\sigma^2, \tag{2}$$

$$\kappa_{\rm eff} = \frac{\kappa_5^2}{6}\epsilon\sigma, \tag{3}$$

are respectively the effective cosmological constant, and the effective gravitational Einstein constant on the brane. The parameter σ is the brane tension. We see that the brane tension regulates the relation between the strength of the gravitational coupling in the

5-dim bulk and in the brane. The crucial correction is the term quadratic in the density, which modifies the dynamics of the scale factor. In the above $\epsilon = \pm 1$ according to whether the extra dimension is spacelike or timelike respectively. The choice $\epsilon = -1$ implements realistic bounces in the dynamics and we require σ to be negative in order that the effective gravitational Einstein constant $\kappa_{\rm eff}$ on the brane be positive and compatible with the observations. The energy scale of the bounce is given by $\rho \sim 2|\sigma|$. Finally since $\epsilon = -1$ a braneworld with $\Lambda_{\rm eff} \geq 0$ must have a positive bulk cosmological constant $\Lambda_5 > 0$. An elegant geometrical derivation of braneworld dynamics embedded in 5-dim spacetimes may be found in [4, 5] where both high energy local corrections and non-local bulk corrections on a Friedmann–Robertson–Walker (FRW) brane are analyzed.

In the present paper our purpose is to examine the dynamics of spatially closed FRW inflationary braneworld models with a minimal set of ingredients, namely, a coupled massive scalar field plus a radiation fluid. These matter fields evolve on the brane, where high energy/quantum gravity corrections due to the bulk are included and implement non-singular bounces. We will restrict ourselves to non-singular bouncing solutions that are oscillatory and bounded, or initially bounded. Such configurations avoid the problem of initial conditions at past infinity occurring with one-single-bounce solutions; furthermore they would be amenable to a straightforward semi-classical treatment. These solutions are in principle stable and would never enter an inflationary phase with an exponential growth of the scale factor since they correspond to periodic orbits of the integrable dynamics in the gravitational sector. It is worth noting that in the realm of general relativity the dynamical behavior of homogeneous and isotropic cosmological models in the presence of a massive scalar field was analytically studied for the first time in the pioneer papers by Starobinsky [6], and by Belinsky, Grishchuk, Zel'dovich and Khalatnikov [7]. Starobinsky examined the possibility of a non-singular model due to quantum corrections of the scalar field near the region of maximum contraction of a $k = 1$ model. Belinsky *et al* used the methods of the qualitative theory of dynamical systems to examine the generality and conditions of realization of inflationary stages of expansion.

In our model the introduction of a massive scalar field, even in the form of small fluctuations, will turn out to have non-integrable dynamics. As a consequence, non-linear resonance phenomena are present in the phase space dynamics for certain domains of the parameter space of the models which we call windows of resonance. The associated dynamical configurations become metastable allowing the orbits escape to the de Sitter infinity in a finite time. The change from stable to metastable is mathematically described as the bifurcation of the periodic orbit of the gravitational sector (in the neighborhood of which the inflaton fluctuations take place) due to the resonance. We organize the paper as follows. In section 2 we describe the model with its minimal sets of ingredients and examine some of the structures of its phase space, such as critical points and the invariant plane, that constitute the skeleton of the dynamics. In section 3 we make a semi-analytical approach to the phenomenon of non-linear resonance, with an accurate approximation for the dominant resonances that allows us to localize and label the dominant resonant windows in the parameter space. Section 4 discusses the physical constraints imposed by the resonances on the parameters of the model in order that inflation may be realized. We also discuss how typical this behavior is and the structural stability of the resonance pattern. Section 5 is dedicated to final discussions and conclusions.

JCAP10(2007)008

2. The model and the phase space dynamics

We consider a braneworld model with a closed Friedmann–Robertson–Walker (FRW) metric embedded in a 5-dim conformally flat bulk with one extra timelike dimension. The model contains a minimal set of ingredients, namely, a conformally coupled scalar field (the inflaton field) ϕ and a radiation fluid, evolving on the brane with corrections due to the bulk. Our task here is to derive the Hamiltonian of the model and characterize its phase space. We start by giving a brief introduction to braneworld theory, making explicit the specific assumptions used in obtaining the dynamics of the model. We rely on references [3]–[5], and our notation basically follows [8]. Let us start with a 4-dim Lorentzian brane Σ with metric g_{ab} embedded in a 5-dim bulk $\mathcal{M}$ with metric g_{AB}. Capital italic indices range from 0 to 4, small italic indices range from 0 to 3. We regard Σ as a common boundary of two pieces $\mathcal{M}_1$ and $\mathcal{M}_2$ of $\mathcal{M}$ and the metric g_{ab} induced on the brane by the metric of the two pieces should coincide, although the extrinsic curvatures of Σ in $\mathcal{M}_1$ and $\mathcal{M}_2$ are allowed to be different. The action for the theory has the general form

$$S = \frac{1}{2\kappa_5}\left[\int_{\mathcal{M}_1}\left({}^{(5)}R - 2\Lambda_5\right) - 2\epsilon\int_\Sigma K_1 + \int_{\mathcal{M}_2}\left({}^{(5)}R - 2\Lambda_5\right) - 2\epsilon\int_\Sigma K_2\right] + \int_\Sigma\left(\frac{1}{2\kappa_4}{}^{(4)}R - 2\sigma\right) + \int_\Sigma L_4(g_{ab},\rho,\phi). \tag{4}$$

In the above ${}^{(5)}R$ is the Ricci scalar of the Lorentzian 5-dim metric g_{AB} on $\mathcal{M}$, and ${}^{(4)}R$ is the scalar curvature of the induced metric g_{ab} on Σ. The parameter σ is called the brane tension. The unit vector n^A normal to the boundary Σ has norm ϵ. If $\epsilon = -1$ the signature of the bulk space is $(-,-,+,+,+)$, so the extra dimension is timelike. The quantity $K = K_{ab}g^{ab}$ is the trace of the symmetric tensor of extrinsic curvature $K_{ab} = Y^C_{,a}Y^D_{,b}\nabla_C n_D$, where $Y^A(x^a)$ are the embedding functions of Σ in $\mathcal{M}$ [3]. Also

$$L_4(g_{ab},\rho,\phi) = \sqrt{-g}\left[\rho + \frac{1}{2}(g^{ab}\phi_{,a}\phi_{,b} - m^2\phi^2) + \frac{\xi}{2}{}^{(4)}R\phi^2\right] \tag{5}$$

is the Lagrangian density of the four-dimensional massive inflaton field ϕ plus a radiation fluid (equation of state $p = \rho/3$), whose dynamics is restricted to the brane Σ. They interact only with the induced metric g_{ab}. We further assume that the inflaton field is non-minimally coupled with g_{ab}, with coupling parameter ξ. All integrations over the bulk and the brane are taken with the natural volume elements $\sqrt{-\epsilon^{(5)}g}\,\mathrm{d}^5x$ and $\sqrt{-{}^{(4)}g}\,\mathrm{d}^4x$ respectively. κ_5 and κ_4 are Einstein constants in five and four dimensions. Throughout the paper we use units such that $\hbar = c = 1$.

Variations that leave the induced metric on Σ intact result in the equations

$${}^{(5)}G_{AB} + \Lambda_5 g_{AB} = 0, \tag{6}$$

while considering arbitrary variations of g_{AB} and taking into account (6) we obtain

$${}^{(4)}G_{ab} + \epsilon\frac{\kappa_4}{\kappa_5}(S^{(1)}_{ab} + S^{(2)}_{ab}) = \kappa_4(\tau_{ab} - \sigma g_{ab}), \tag{7}$$

where $S_{ab} \equiv K_{ab} - Kg_{ab}$ and τ_{ab} is the energy–momentum tensor of matter and fields

on the brane. In the limit $\kappa_4 \to \infty$ equation (7) reduces to the Israel–Darmois junction condition [9]

$$(S^{(1)}_{ab} + S^{(2)}_{ab}) = \epsilon\kappa_5(\tau_{ab} - \sigma g_{ab}). \tag{8}$$

We impose the Z_2-symmetry [5] and use the junction conditions (8) to determine the extrinsic curvature on the brane,

$$K_{ab} = -\frac{\epsilon}{2}\kappa_5\left[\left(\tau_{ab} - \frac{1}{3}\tau g_{ab}\right) + \frac{\sigma}{3}g_{ab}\right]. \tag{9}$$

Now using the Gauss equation ${}^{(4)}R_{abcd} = {}^{(5)}R_{MNRS}Y^M_{,a}Y^N_{,b}Y^R_{,c}Y^S_{,d} + \epsilon(K_{ac}K_{bd} - K_{ad}K_{bc})$ together with equations (6) and (9) we arrive at the induced field equations on the brane

$${}^{(4)}G_{ab} = -\left(\Lambda_5 + \frac{1}{12}\kappa_5^2\epsilon\sigma^2\right)g_{ab} + \frac{\kappa_5^2}{6}\epsilon\sigma\tau_{ab} + \epsilon\kappa_5\pi_{ab}. \tag{10}$$

In the above

$$\pi_{ab} = -\tfrac{1}{4}\tau_{ac}\tau^c_b + \tfrac{1}{12}\tau\tau_{ab} + \tfrac{1}{8}g_{ab}\tau_{cd}\tau^{cd} - \tfrac{1}{24}g_{ab}\tau^2. \tag{11}$$

We remark the absence of the conformal tensor projection in equation (10) since the FRW brane is embedded in a conformally flat bulk.

Equation (10) is the dynamical equation of the gravitational field on the brane. It is similar to Einstein equations in four dimensions, except in the second term in the RHS which is a correction resulting from the brane–bulk interaction quadratic in the extrinsic curvature. Another important difference is that the effective Newton's gravitational constant $G_N = (\kappa_5^2\sigma\epsilon/48\pi)$ as well as the effective cosmological constant in the brane depend basically on the brane tension σ, as we will discuss. We recall that for the evaluation of the extrinsic curvature (9) we use the energy–momentum tensor of the matter fields on the brane. In our model they are described by the Lagrangian density (5). Since only small spatially homogeneous fluctuations of ϕ will be taken into account (they are used just to trigger the resonances) we will assume that the bulk corrections arising from the extrinsic curvature are dominated by the radiation fluid and the brane tension σ only. In this instance we have

$$\pi_{ab} = \tfrac{2}{9}\rho^2 \mathrm{u}_a \mathrm{u}_b + \tfrac{5}{36}\rho^2 g_{ab}, \tag{12}$$

where ρ is the density of the radiation fluid as measured by an observer with 4-velocity field u_a. Therefore in our model—where the extra dimension is timelike ($\epsilon = -1$)—the bulk corrections behave effectively as a phantom fluid with negative energy density.

Let us consider the closed FRW metric on the brane given by the line element

$$\mathrm{d}s^2 = N(t)^2\,\mathrm{d}t^2 - a(t)^2\left[\frac{\mathrm{d}r^2}{1 - kr^2} + r^2(\mathrm{d}\theta^2 + \sin^2\theta\,\mathrm{d}\phi^2)\right], \tag{13}$$

where $a(t)$ is the scale factor and $N(t)$ is the lapse function. In view of the above, the effective Lagrangian density that describes the dynamics (10) for our model is given by

$$L = -\sqrt{-g}[-R/2(1 - \xi\phi^2) - \Lambda_{\mathrm{eff}} + \tfrac{1}{2}(g^{ab}\phi_{,a}\phi_{,b} - m^2\phi^2) - \tilde{\rho}], \tag{14}$$

where

$$\Lambda_{\mathrm{eff}} = (\Lambda_5 + \tfrac{1}{12}\kappa_5^2\epsilon\sigma^2) \tag{15}$$

and

$$\tilde{\rho} = \frac{\kappa_5^2 \epsilon}{12}(2\sigma\rho + \rho^2). \tag{16}$$

We notice that $\tilde{\rho}$ is obtained as the component $(0,0)$ of the last two terms in the RHS of (10). The Lagrangian (14) corresponds to (5) properly modified. The non-minimal coupling of the inflaton with gravitation considered here is partly motivated by quantum calculations in curved spacetimes (taking into account quantum backreaction, renormalization, etc) and partly by the possibility of constructing successful inflationary and pre-inflationary scenarios [10]. The case $\xi = 0$ is the usual minimal coupling of the scalar field with gravitation, and $\xi = 1/6$ is the so-called conformal coupling [11].

In the above, g is the determinant of the metric and R is the Ricci scalar given by

$$R = -\frac{6}{N^2}\left(\frac{\ddot{a}}{a} + \frac{\dot{a}^2}{a^2} + N^2\frac{k}{a^2} - \frac{\dot{a}\dot{N}}{aN}\right). \tag{17}$$

Due to the spatial homogeneity of the model, the total action can then be expressed as

$$S = V_0 \int \mathrm{d}t\, N a^3 \left[-\frac{R}{2}(1-\xi\phi^2) + \frac{1}{2N^2}\dot{\phi}^2 - \Lambda_{\mathrm{eff}} - \frac{m^2}{2}\phi^2 - \tilde{\rho}\right], \tag{18}$$

where the constant $V_0 = 4\pi(\arcsin\sqrt{k})/\sqrt{k}$ stands for the volume of the spatial sections $t = \text{const}$. Discarding the total time derivative term in the integrand of (18), and further introducing a new scalar field variable $\varphi = \phi a^{6\xi}$, equation (18) turns into

$$\begin{aligned} S = V_0 \int \mathrm{d}t \Bigg[&-\frac{3a\dot{a}^2}{N} + 3kaN + \frac{a^{(3-12\xi)}}{2N}\dot{\varphi}^2 + \frac{3\xi(1-6\xi)}{N}\dot{a}^2 a^{(1-12\xi)}\varphi^2 \\ &- Na^3\left(\Lambda_{\mathrm{eff}} + \frac{m^2}{2}\varphi^2 a^{-12\xi}\right) - 3k\xi N\varphi^2 a^{(1-12\xi)} - Na^3\tilde{\rho}\Bigg]. \end{aligned} \tag{19}$$

By a proper rescaling of the scale factor we set $V_0 = 1$. From the kinetic terms of (19) we define the momenta canonically conjugate to a and φ respectively as

$$\begin{aligned} p_a &= -\frac{6a\dot{a}}{N} + \frac{6\xi(1-6\xi)}{N}\dot{a}\varphi^2 a^{(1-12\xi)}, \\ p_\varphi &= \frac{a^{(3-12\xi)}}{N}\dot{\varphi}, \end{aligned}$$

so that (19) assumes the canonical form

$$S = \int \mathrm{d}t\,(\dot{a}p_a + \dot{\varphi}p_\varphi - NH), \tag{20}$$

where

$$\begin{aligned} H = &\frac{p_a^2}{12a[-1+(1-6\xi)\xi\varphi^2 a^{-12\xi}]} + \frac{p_\varphi^2}{2a^{(3-12\xi)}} - 3ka \\ &+ a^3\left(\Lambda_{\mathrm{eff}} + \frac{m^2}{2}\varphi^2 a^{-12\xi}\right) + 3k\xi\varphi^2 a^{(1-12\xi)} + a^3\tilde{\rho}. \end{aligned} \tag{21}$$

JCAP10(2007)008

Extremizing the action (20) with respect to variations in N results in the Hamiltonian constraint

$$H = \frac{p_a^2}{12a[-1+(1-6\xi)\xi\varphi^2 a^{-12\xi}]} + \frac{p_\varphi^2}{2a^{(3-12\xi)}} - 3ka + a^3\left(\Lambda_{\rm eff} + \frac{m^2}{2}\varphi^2 a^{-12\xi}\right) + 3k\xi\varphi^2 a^{(1-12\xi)} + a^3\tilde{\rho} = 0. \tag{22}$$

Partly due to analytical simplicity of the analysis of non-linear resonance phenomena, in the remainder of the paper we will restrict ourselves to the dynamics in the conformal coupling case $\xi = 1/6$. For an extended range of values of ξ, a larger parameter space analysis is demanded and will be the object of a future investigation. Adopting the conformal time gauge $N = a$, the dynamics of the model may then be derived from the Hamiltonian constraint expressed in the form

$$H = \frac{1}{12}p_a^2 - a^4\Lambda_{\rm eff} + 3ka^2 - \frac{1}{2}(p_\varphi^2 + \varphi^2) - \frac{1}{2}m^2a^2\varphi^2 - a^4\frac{\epsilon\kappa_5^2}{12}(2\sigma\rho + \rho^2) = 0. \tag{23}$$

We remark that this Hamiltonian coincides with equation (18) of the second reference [3] (in the gauge $N = 1$, with the identification $M^3 = 2/\kappa_5$), up to the presence of a conformally coupled scalar field. In the FRW geometry (13) the energy density of the radiation fluid is given by $\rho = E_0 a^{-4}$ where E_0 is a constant proportional to the total energy of the fluid. We choose $\epsilon = -1$ which implements realistic bounces in the model; as a consequence we require σ to be negative. We also rescale $k = 1$. Substitution in (23) results in

$$H = \frac{1}{12}p_a^2 + V(a) - \frac{1}{2}(p_\varphi^2 + \varphi^2) - \frac{1}{2}m^2a^2\varphi^2 - 2\frac{\kappa_5^2}{12}|\sigma|E_0. \tag{24}$$

In the above $V(a)$ is a potential in the gravitational sector (a, p_a) given by

$$V(a) = 3a^2 - \Lambda_{\rm eff}a^4 + \frac{\kappa_5^2}{12}E_0^2\frac{1}{a^4}, \tag{25}$$

displaying the contributions of the spatial curvature term, the effective cosmological constant and the correction term arising from the bulk geometry responsible for the bounces. The quantity $\kappa_5^2|\sigma|E_0/6 \equiv \kappa_{\rm eff}E_0$ is the Hamiltonian constant of motion, and corresponds to the total mass–energy of the radiation fluid given in geometrical units, scaled by $|\sigma|\kappa_5^2$ which parametrizes the effective gravitational coupling in the brane. The parameter σ will be a crucial component of the parametric space of the system labeled by (m, E_0, σ), the independent variation of which will determine regions of parametric resonance as well as regions of parametric stability of the dynamics, for fixed m and E_0. As a consequence the effective gravitational constant will have distinct values in configurations of the system where escape to inflation is allowed.

In the low energy limit the cosmological constant $\Lambda_{\rm eff}$ may be interpreted as the effective vacuum energy of the inflaton field and the φ are the spatially homogeneous expectation values of the inflaton fluctuations about its vacuum state. For numerical purposes we fix $\kappa_5^2/12 = 1$ and we will drop the subscript 'eff' from the effective cosmological constant on the brane.

JCAP10(2007)008

The final form of the Hamiltonian to be discussed in the remainder of the paper is then

$$\mathcal{H} = \frac{1}{12}p_a^2 + 3a^2 - \Lambda a^4 + \frac{E_0^2}{a^4} - \frac{1}{2}(p_\varphi^2 + \varphi^2) - \frac{1}{2}m^2a^2\varphi^2 - 2|\sigma|E_0 = 0. \quad (26)$$

The focus on the underlying bulk–brane structure of the gravitational dynamics will lead us to label the parameter space of the system with (m, E_0, σ).

We start by giving an overview of the basic skeleton of phase space, which organizes the whole dynamics of the model. We note first that the Hamiltonian (26) is separable, and consequently integrable, for $m = 0$. A non-zero mass couples the two degrees of freedom (the gravitational sector and the scalar field sector), turning the system non-integrable. The critical points (stationary solutions of the Hamilton's equations derived from (26)) in the finite region of phase space are characterized by

$$p_a = p_\varphi = 0, \qquad \varphi = 0, \qquad V'(a) = 0; \quad (27)$$

and are connected to the extrema of the potential $V(a)$. In the region $a \geq 0$ there are only two critical points, P_0 and P_1, associated with the maximum and minimum of the potential, respectively. P_0 corresponds to the configuration of the Einstein static universe while the critical point P_1 is a stable static solution arising as a consequence of the effective negative energy density connected to the bulk–brane corrections to the gravitational dynamics. P_0 is a saddle center and P_1 a pure center, as can be seen from the linearization of the dynamics about each critical point [12].

A careful analysis of the potential $V(a)$ shows that the energy of the critical points P_0 and P_1 is always greater than zero, namely, $V(P_0) > 0$ and $V(P_1) > 0$. Furthermore the presence of both critical points depends crucially on a relation between Λ and E_0: for a given Λ the value of E_0 such that both critical points are present is limited by

$$E_0^2(\text{max}) = \frac{2187}{4096}\frac{1}{\Lambda^3}. \quad (28)$$

Namely, if $E_0^2 > E_0^2(\text{max})$ we have $V'(a) < 0$ for all $a > 0$, implying that no critical points exist in the finite phase space domain.

The critical points are contained in a two-dimensional submanifold of the phase space, called the invariant plane and defined by

$$\varphi = 0, \qquad p_\varphi = 0. \quad (29)$$

Orbits with initial conditions on this plane are totally contained in it, actually corresponding to the dynamics in the sector (a, p_a) of the separable case $m = 0$. The phase portrait in the invariant plane is depicted in figure 1(b), connected to the one-dimensional motion in the potential $V(a)$. Due to the character of fluctuations of φ, physical configurations are the ones corresponding to initial conditions near the invariant plane.

Also, a straightforward analysis of the infinity of phase space shows the presence of a pair of critical points in this region, one acting as an *attractor* (stable de Sitter configuration) and the other as a *repeller* (unstable de Sitter configuration).

The model allows for the presence of perpetually bouncing universes in the invariant plane (cf figure 1(b)). We remark that the smaller Λ, the larger the phase space domain available for bouncing orbits; in contrast, if the cosmological constant increases while E_0 is maintained fixed the domain of phase space available for these bouncing solutions

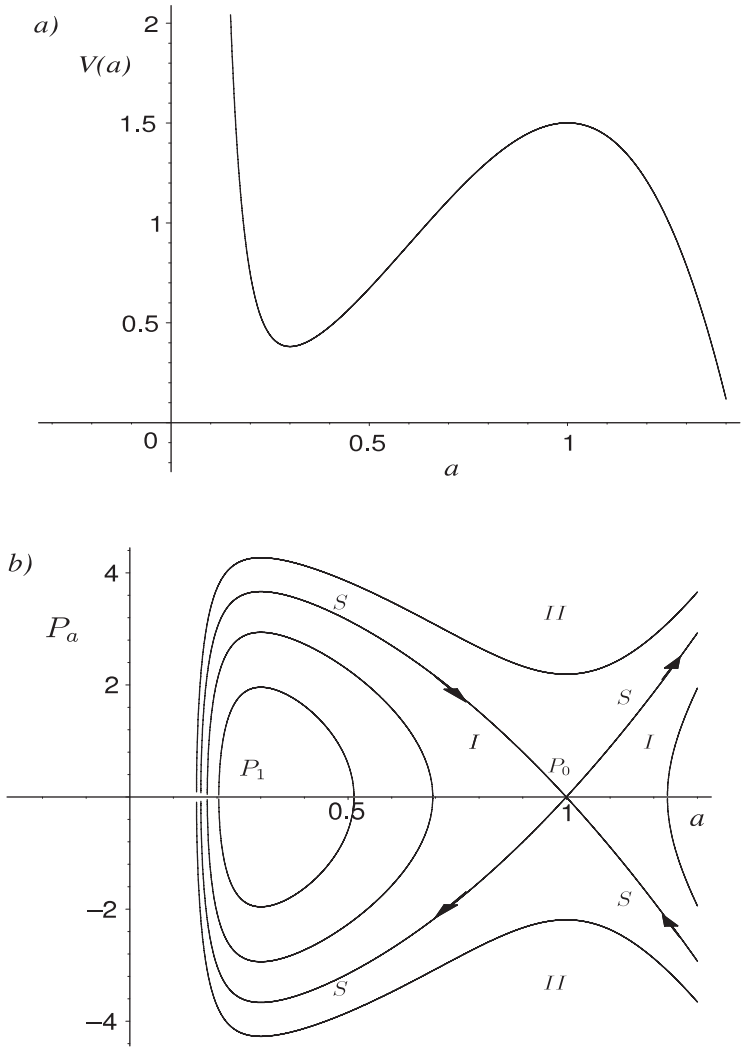

Figure 1. (a) Plot of the potential $V(a)$ for positive Λ, and (b) the phase portrait of the invariant plane with the critical points P_0 and P_1.

decreases; beyond a certain value of Λ fixed by equation (28) only solutions with one single bounce are possible. The latter have a behavior analogous to the integrable solutions shown in the phase portrait of figure 1(b) for $|\sigma|E_0 > E_{P_0}$, where $E_{P_0} \equiv V(P_0)$ is the value of the Hamiltonian constant for the saddle center P_0.

As we mentioned already, we will restrict ourselves to dynamical configurations with initial conditions for which the universe undergoes a series of bounces before it enters an inflationary regime. They represent a hypothetical pre-inflationary phase where the terms arising from high energy corrections play the fundamental role of preventing the initial singularity, and produce a non-trivial dynamics before the exit to inflation[4]. These configurations are basically the ones for which $2|\sigma|E_0 < E_{P_0}$. They have the theoretical

[4] The exit to inflation occurs whenever a given orbit approaches asymptotically the de Sitter configuration; the inflationary phase is characterized by the de Sitter configuration driven by the effective cosmological constant understood as part of the scalar field, as its vacuum energy is dominant during inflation.

advantage over one-single-bounce models in that they avoid the problem of initial conditions at past infinity; furthermore they would be amenable to a straightforward semi-classical treatment. Values of $2|\sigma|E_0 < E_{P_0}$ actually correspond to bounded motions in the integrable case $m = 0$, or to initially bounded motion in the non-integrable cases when stable configurations may be disrupted by non-linear resonance phenomena. Windows of resonance in the parameter space (m, E_0, σ) favor inflation since the resonances destroy KAM tori that trap the orbits about the origin $(\varphi = 0, p_\varphi = 0)$. Among other complex dynamical phenomena, non-linear resonances may create structures such as Cantori that favor inflation after a process of long time diffusion. We have recently dealt with analogous phenomena in a cosmological scenario with a phantom fluid having $\rho_{\rm ph} \sim -1/a^6$ [13]. The analysis there will be briefly reviewed in the next section as applied to the system (26), in order that we can examine properly one of the main questions of the paper, namely the physical constraints that non-linear resonance phenomena impose on the brane tension parameter, the mass of the inflaton and E_0. As we will see, only very narrow windows in the parameter space will allow for phase space configurations that realize inflation.

3. The non-linear resonance windows: a semi-analytical approach

Let us consider the dynamics in the energy surface $2|\sigma|E_0$ corresponding to a bounded motion in the integrable case $m = 0$, or to initially bounded motion in the non-integrable cases.

We start from the integrable case $m = 0$ in which the motion is separable with the separately conserved quantities $E_a = p_a^2/12 + V(a)$ and $E_\varphi = (p_\varphi^2 + \varphi^2)/2$, satisfying $2|\sigma|E_0 = -E_\varphi + E_a$. For $E_a < E(P_0)$ it is not difficult to see that the equation $E_a - V(a) = 0$ has three real positive roots $(a_3 < a_2 < a_1)$ in the physical domain $a > 0$, and two conjugate imaginary roots $\pm i\alpha$. For the non-integrable case $m^2 \neq 0$, with m small and/or initial conditions φ_0 small, $E_a \simeq 2|\sigma|E_0$ and the period of the associated periodic orbit is given approximately by

$$T_a = \sqrt{\frac{3}{\Lambda}} N, \tag{30}$$

where N is the complete elliptic integral of the third kind [14]

$$N = \int_{a_3^2}^{a_2^2} \frac{\sqrt{x}\,\mathrm{d}x}{\sqrt{(x+\alpha^2)(x-a_3^2)(x-a_2^2)(x-a_1^2)}}. \tag{31}$$

The associated frequency is defined as

$$\nu_a = 1/T_a, \tag{32}$$

such that the angle variable $\Theta_a = \nu_a \tau$ varies in the interval $[0, 1]$ during a complete cycle of the original variable a. In the sector (φ, p_φ) the frequency in the non-integrable case may be approximated by[5]

$$\tilde{\nu}_\varphi = \frac{1}{2\pi}\sqrt{1 + \frac{m^2}{2}(a_2^2 + a_3^2)}. \tag{33}$$

[5] The correction of $\nu_\varphi = 1/2\pi$ into $\tilde{\nu}_\varphi$ in equation (33) is obtained by using the exact equation $\ddot{\varphi} + (1 + m^2 a^2(\tau))\varphi = 0$ and substituting in it the solution $a(\tau)$ of the associated integrable case and extracting the dominant correction. This gives an accurate approximation that is very efficient for localizing the resonances, as shown in figure 2.

For future reference, we note that the periodic orbits of the sector (a, p_a), in the integrable case, will be represented by the elliptic fixed point $(\varphi = 0, p_\varphi = 0)$ of the Poincaré map with surface of section $p_a = 0$. For m small this picture is maintained with $(\varphi = 0, p_\varphi = 0)$ as a center of a primary island of invariant KAM tori; in fact, for a small coupling parameter m, the KAM theorem [15] establishes the stability of tori with a sufficiently incommensurate frequency ratio, which in the present case means ν_a sufficiently irrational. Other integrable tori are destroyed by the non-integrable perturbation, and the region between two remaining invariant tori presents an intricate dynamics (unstable periodic orbits, stable periodic orbits surrounded by islands, broken separatrices and stochastic layers, this structure repeating down to smaller scales [16]). However this dynamics is bounded by the two invariant tori with irrational ν_a implying in a certain sense the stability of the dynamics. As m increases numerical experiments show that invariant KAM tori may be destroyed leading to a loss of the stability of the system. This is the case of interest to us as orbits initially trapped about the center $(\varphi = 0, p_\varphi = 0)$ can escape into an inflationary phase. An important mechanism for this break-up of invariant tori is non-linear resonance [17], a phenomenon that occurs in a restricted domain of the parameters, as we proceed to discuss.

Approximate analytical treatment analogous to that of [13] shows that the dominant resonances of the system are determined by

$$R \equiv \frac{\nu_a}{\tilde{\nu}_\varphi} = \frac{2}{n}, \qquad n \geq 2. \tag{34}$$

For a fixed integer $n \geq 2$, equation (34) determines surfaces in the parameter space (m, E_0, σ), in the neighborhood of which an n-resonance occurs. The setting up of the resonance is signaled by the bifurcation of the stable periodic orbit at the origin $(\varphi = 0, p_\varphi = 0)$ into an unstable periodic orbit plus one or two characteristic stable periodic orbits of the resonance, according respectively to whether n is odd or even. The condition $n \geq 2$ guarantees that the mass m is real for values of $2|\sigma|E_0$ corresponding to initially bounded orbits.

The actual resonant chart is now constructed numerically using the exact dynamics. The expression (34)—where approximations as well as the neglect of non-resonant terms were used—constitutes an accurate guide for localizing and labeling the resonances. However in the actual resonance chart constructed numerically with the exact dynamics the surfaces will be spread into small finite volumes; these volumes are called *windows of resonance* for the exact dynamics. In the numerical experiments of the paper we adopted $\Lambda = 3/2$ for computational convenience. The stability of the results with respect to the variation of Λ is discussed in section 4.

In figure 2 we display the resonance chart in the parametric plane (m, σ) for $\Lambda = 3/2$ and $E_0 = 0.013$. The chart corresponds to initial conditions taken near the invariant plane, with $p_a = p_\varphi = 0$, $\varphi = 10^{-4}$. The continuous lines are solutions of equation (34) while the gray regions spreading about the lines are the sections of the resonance windows by the plane $E_0 = 0.013$. The remaining regions (white) of the parameter space correspond to otherwise stable motion (namely motion between two KAM tori). On driving the configuration of the system towards a resonance zone in the parametric space we turn a stable configuration into a metastable one with possible disruption of orbits and escape towards the de Sitter infinity in a finite time.

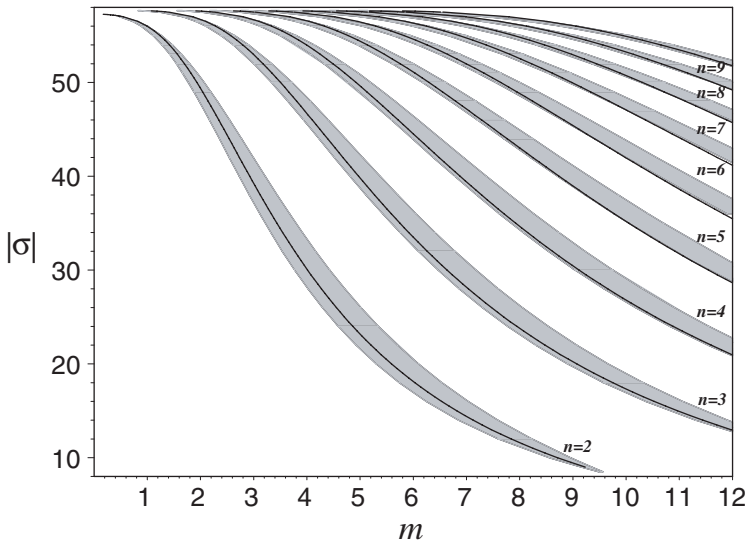

Figure 2. Resonance chart of the exact dynamics in the parameter plane (m, σ) for $E_0 = 0.013$ and $\varphi_0 = 10^{-4}$. The continuous lines are solutions of the approximate resonant condition (34), while the gray regions about the continuous lines correspond to parametric domains of resonance for the exact dynamics, with bifurcation of the periodic orbit at the origin. The white regions correspond to stable motion.

It is worth noticing that the resonance windows are bounded above and below, a feature independent of the value of Λ. For resonances $n \geq 2$ the theoretical upper bound for σ obtained from equation (34) results in $\sigma_{\rm upper} \simeq -57.75$; for the resonance $n = 2$ however we obtain a smaller upper bound $\sigma_{\rm upper} \simeq -57.294$ corresponding to the minimum value of $m \simeq 0.034\,575\,550$. The lower bound $\sigma_{\rm lower} \simeq -8.35$ results for all n resonances. These numerical values were obtained for $\Lambda = 3/2$ adopted in our numerical experiments. The upper and lower bounds for σ and the lower bound for m are associated with the existence of the three real roots (a_3, a_2, a_1) of the polynomial $E_a - V(a) = 0$, where $E_a \simeq 2|\sigma|E_0$, and consequently with the existence of initially bouncing motion.

From the point of view of pre-inflationary models, stability versus non-linear resonance instability will be considered connected to initial conditions near the invariant plane only, namely with φ, p_φ small, corresponding to fluctuations of the inflaton field. Non-linear resonance will turn orbits generated from these initial conditions from stable to unstable (and vice versa) as a consequence of bifurcation of the critical point $\varphi = p_\varphi = 0$, at the origin of the Poincaré map with surface of section $p_a = 0$, from a center to a saddle (and vice versa). We recall that the origin of the map is a periodic orbit of period T_a in the (a, p_a) sector.

Analogous schematic analysis of the dynamics near the resonances is given in [13]. The basic pattern that emerges as the system enters a resonance window is a characteristic structure of stable periodic orbits, associated with the particular resonance n. These periodic orbits are enclosed by KAM tori and the primary islands of KAM dynamics have a border beyond which the dynamics is stochastic, filling large domains of phase space.

JCAP10(2007)008

Table 1. Classification of resonances according to the characteristic periodic orbits.

Resonance	Characteristic periodic orbits	Primary KAM islands, section $\varphi = 0$	Primary KAM islands, section $p_a = 0$
$n = 2k$	2	k	1
$n = 2k + 1$	1	$2k + 1$	2

This is the general picture but some remarkable differences appear according to whether the resonance is odd or even, namely, $n =$ odd or even. These results are summarized in table 1.

In table 1, for even resonances $n = 2k$, the number k of primary KAM islands in the surface of section $\varphi = 0$ refers to each characteristic periodic orbit.

We should remark that in a given surface of constant Hamiltonian, namely $2|\sigma|E_0 =$ const, a family of invariant KAM tori is present about each characteristic periodic orbit. However, according to the above table, the number of invariant tori in the case of $n =$ even resonances is twice the number of invariant tori in the case of $n =$ odd resonances; so for an $n =$ even resonance two distinct invariant tori (each about one of the two distinct characteristic periodic orbits of the resonance) may end up with the same energy (they differ by $\varphi \to -\varphi$). This *degeneracy* in the classical configuration may be raised in a quantum version of the bounded dynamics with possible tunneling between these two classically allowed regions, with the quantum state having a non-null amplitude on both tori. Therefore the expected tunnelings enhanced by resonances between the classically allowed regions inside and outside the well of figure 1(a) do not have to be treated separately, in an eventual quantum version of the dynamics.

4. Resonance bifurcations and physical constraints on the parameters of the model

Let us consider a fixed value of the Hamiltonian constant of motion $2|\sigma|E_0$ in the resonance chart of figure 1(a). For values of m not in the resonance windows, the origin $(\varphi = 0, p_\varphi = 0)$ of the Poincaré map with surface of section $p_a = 0$ is a center connected to a stable periodic orbit in the sector (a, p_a). However as the system is driven into a given resonance window by an appropriate change of m and/or σ this stable periodic orbit bifurcates into an unstable periodic orbit, namely the origin of the Poincaré map turns into a saddle.

The instability versus the stability of the origin $(\varphi = 0, p_\varphi = 0)$ is crucial for the dynamics of inflation (namely, the escape to inflation), having a bearing on the dynamics of the spatially homogeneous expectation values $\varphi(\tau)$ of the inflaton field, related to the escape into inflation. In this instance the initial conditions for φ are assumed to be small, and are to be taken near the invariant plane $\varphi = 0, p_\varphi = 0$, which corresponds to a neighborhood of the critical point of the map at the origin $(\varphi = 0, p_\varphi = 0)$. Therefore the region of parametric stability is unfavorable for producing inflation since the orbit (a configuration of the early universe) will be trapped in a stable state enclosed by two invariant tori of a main KAM island of the map. On the other hand, if the system is in the region of parametric resonance, orbits with initial conditions near the invariant plane

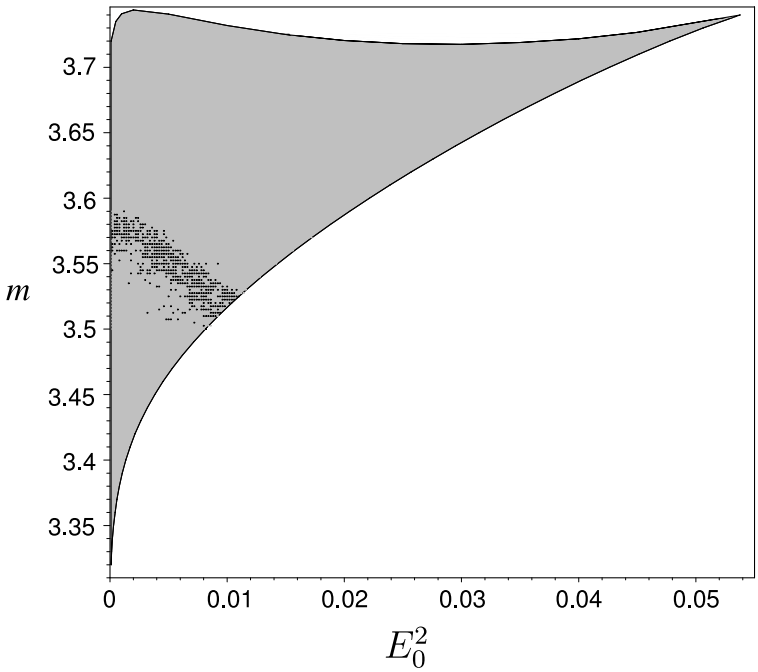

Figure 3. Resonance tongue $n = 3$ (in gray) in the parameter plane (m, E_0^2) for $2|\sigma|E_0 = 1.3$. The heavy black dotted sheet dividing the tongue constitutes a threshold region between disruptive resonances with rapid escape to inflation ($\tau \leq 15\,000$, lower portion of the resonance tongue) and long time diffusion with no escape to inflation (up to $\tau = 100\,000$, upper part of the resonance tongue). Configurations on the threshold correspond to orbits which escape to inflation in a time $15\,000 \leq \tau \leq 100\,000$. Points in the upper part of the tongue correspond to a diffusion dynamics with no escape to inflation, in spite of the bifurcation of the origin (cf text).

are metastable configurations that either escape rapidly to de Sitter infinity or undergo a long time diffusion through stochastic regions of phase space before finally escaping (cf figures 4 and 5 and discussions below).

The resonance windows in the complete parameter space (m, E_0, σ) are constituted of n disjoint 3-dim volumes, the section of which with the plane $E_0 = 0.013$ results in the n shaded regions of figure 2. The volumes of the windows are small as compared to the whole volume of the parameter space, and only initial configurations inside them may realize inflation.

From the point of view of the dynamics of inflation, the resonance windows present a further *structure* connected with disruptive resonances and/or long time diffusion before escape to inflation. In fact, as we proceed to discuss, a considerable domain of the resonance windows—although corresponding to a bifurcation of the stable periodic orbit at the origin—does not lead to escape into inflation and must be properly discarded.

To illustrate this further restriction it will be more appropriate to consider the resonant chart in the parameter plane (E_0, m) for $|\sigma|E_0 = \text{const}$. Without loss of generality, we restrict our analysis to the resonance tongue $n = 3$, shown as the gray region in figure 3, obtained for $2|\sigma|E_0 = 1.3$. As mentioned before, this resonance domain

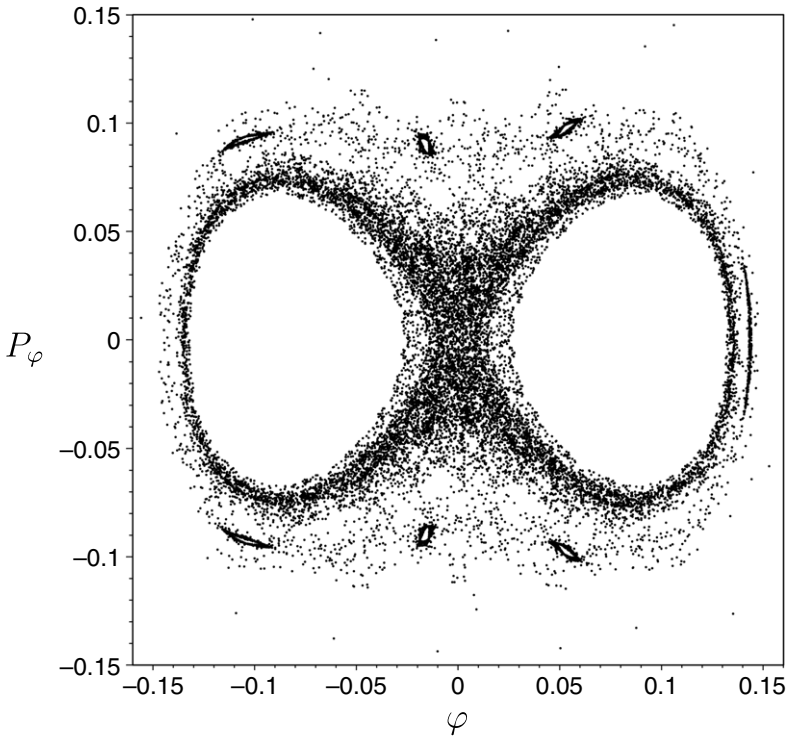

Figure 4. Poincaré map with surface of section $p_a = 0$ for a single orbit generated with initial conditions $p_a = 0 = p_\varphi$, $\varphi = 10^{-4}$, and parameters $(m = 3.572, E_0^2 = 0.002)$ in the threshold region of the $n = 3$ resonance tongue of figure 3. This configuration corresponds to a long time diffusion of the orbit before escape to inflation at $\tau \simeq 76\,300$. The Poincaré map exhibits the structure of the random motion of the orbit in the stochastic sea surrounding primary and secondary KAM islands of the resonance.

JCAP10(2007)008

is numerically constructed considering $n = 3$ bifurcations of the periodic orbit at the origin. However a bifurcation does not necessarily correspond either to a disruptive resonance or to a long time diffusion, both with escape of the orbit to the de Sitter infinity. Actually for large parts of the resonance window the configurations with initial conditions about the origin $(\varphi = 0, p_\varphi = 0)$ remain trapped between two invariant tori of the main KAM islands of the characteristic periodic orbits of the resonance.

Indeed a careful numerical examination shows that in the resonance tongue $n = 3$ of figure 3 we have three dynamically distinct regions. The heavy black dotted sheet that divides the tongue constitutes a *threshold* region in which the resonance induces the escape of orbits in a time $15\,000 \leq \tau \leq 100\,000$, the larger times corresponding to a long time diffusion before escape to inflation. The region below this threshold (at the lower part of the tongue) corresponds to configurations for which the dynamics is highly unstable, the resonances being disruptive with a rapid escape to inflation ($\tau \leq 15\,000$). The region above the threshold (at the upper part of the tongue) corresponds to configurations with chaotic motion bounded between two KAM tori, but otherwise stable. We should note that the borders of the threshold are not sharply defined (possibly with a fractal structure), whatever its limits $\Delta\tau$ of definition.

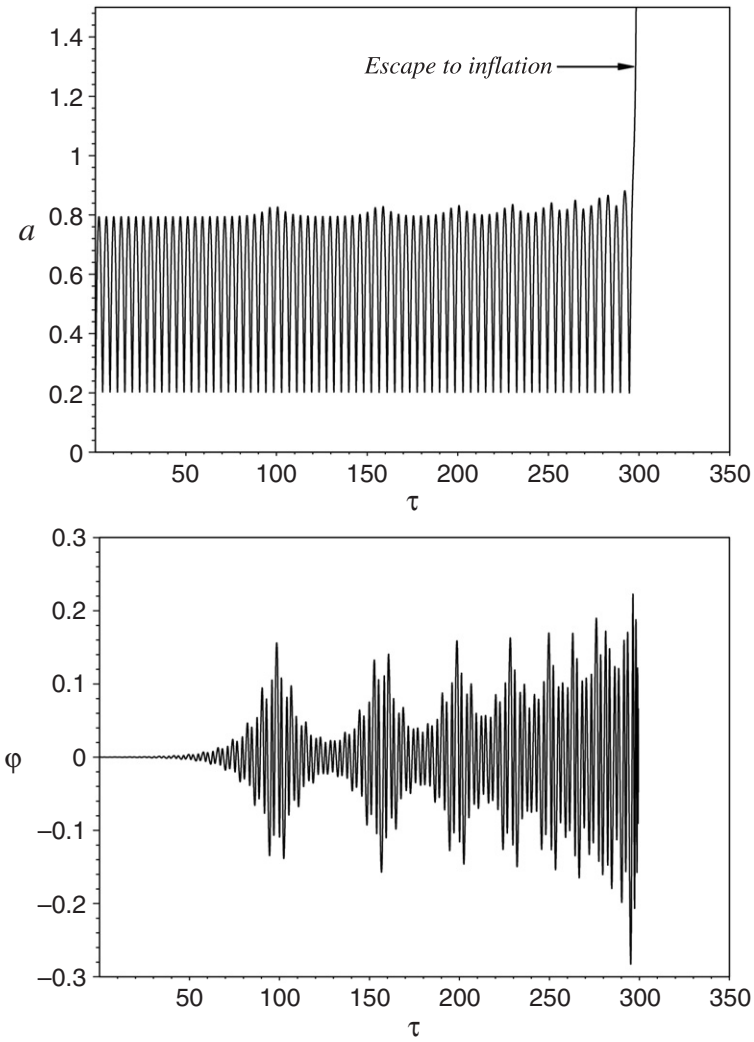

Figure 5. Time signals $a(\tau)$ and $\varphi(\tau)$ for parameters $(m = 3.505, E_0^2 = 0.002)$ below the threshold region of the $n = 3$ resonance tongue of figure 3, corresponding to a disruptive resonance with escape to inflation at $\tau \simeq 300$. The orbit was generated from initial conditions $p_a = 0 = p_\varphi$, $\varphi = 10^{-4}$.

The three dynamically distinct behaviors are illustrated in figures 4–6. Figure 5 displays the time signals $a(\tau)$ and $\varphi(\tau)$ for values $(m = 3.505, E_0^2 = 0.002)$ taken in the region of disruptive resonances, of the tongue $n = 3$ in figure 3. The escape to inflation occurs in $\tau \simeq 300$ and time signals are used since there is not enough recurrence for constructing a well defined Poincaré map. On the other hand figure 4 displays the Poincaré map of a single orbit with initial conditions $p_a = 0 = p_\varphi$ and $\varphi = 10^{-4}$ and corresponding to values $(m = 3.572, E_0^2 = 0.002)$ in the threshold region, with a long time diffusion before escape to inflation. The Poincaré map exhibits the structure of the random motion in the stochastic sea surrounding KAM islands, before the escape at $\tau \simeq 76\,300$. Finally figure 6 shows the time signals of orbits with $(m = 3.65, E_0^2 = 0.02)$ in the upper region of the resonance tongue, corresponding to bounded chaotic motion

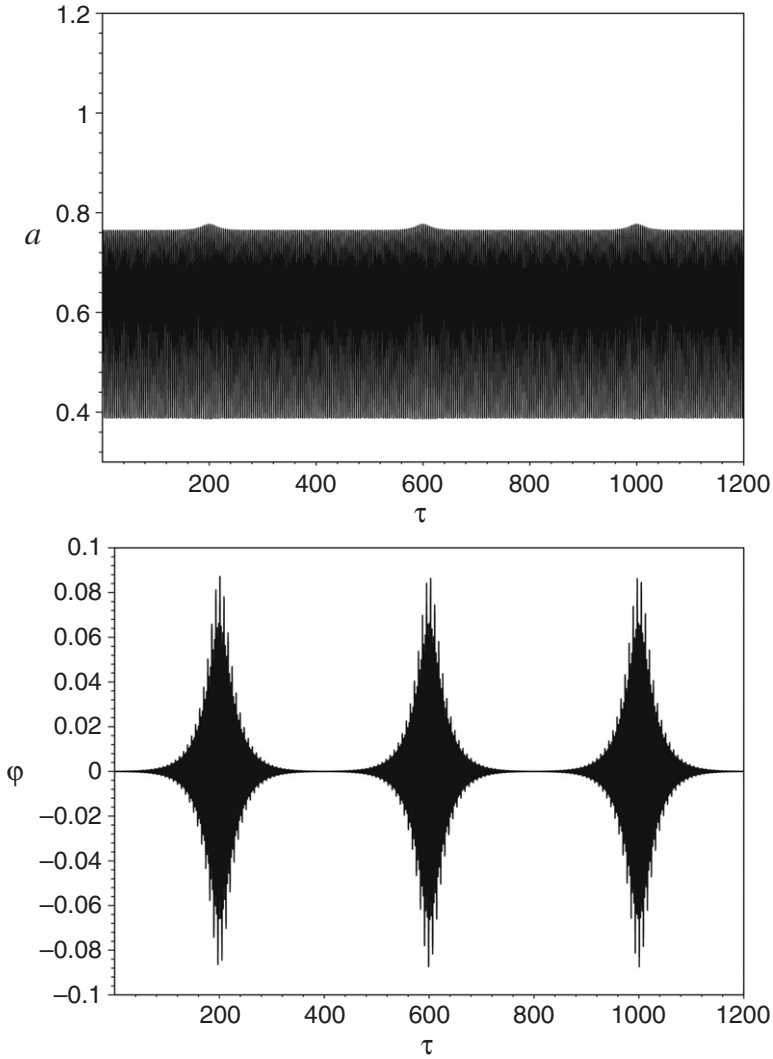

Figure 6. Time signals $a(\tau)$ and $\varphi(\tau)$ for parameters $(m = 3.65, E_0^2 = 0.02)$ in the upper region (above the threshold) of the $n = 3$ resonance tongue of figure 3, corresponding to chaotic stable motion trapped between two KAM tori, with no escape to inflation. The orbit was generated from initial conditions $p_a = 0 = p_\varphi$, $\varphi = 10^{-4}$.

between two KAM tori. We note that the resonance tongue of figure 3 was constructed with $\varphi_0 = 10^{-4}$.

Therefore, from the point of view of the dynamics of inflation, the region of resonance tongue $n = 3$ lying above the threshold and below the upper border of the tongue should also be excluded, as such parameter configurations do not properly realize inflation. The same considerations apply to all n-resonance tongues. The general picture is that bouncing braneworld models have a very restricted domain in their parameter space where inflation can be realized.

The structure of resonance windows imposes some interesting restrictions on the brane tension σ that regulates the gravitational coupling strength on the brane as induced by

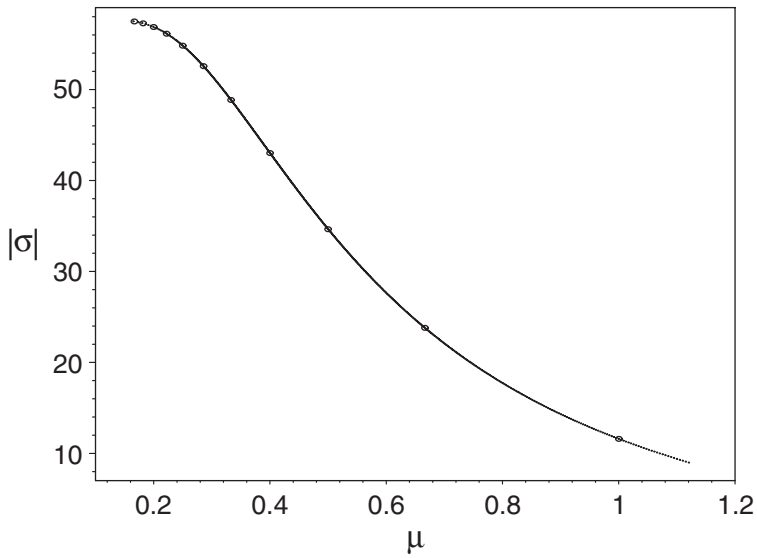

Figure 7. Plot of the brane tension σ versus μ (cf equation (35)) for fixed $m = 8$ and $E_0 = 0.013$. The discrete white dots correspond to values $\mu = 2/n$, for $n = 2$–12. We see that the larger the resonance, the stronger the gravitational interaction on the braneworld inflated from the resonance considered. The discrete values of σ accumulate towards an upper bound for increasing n.

the gravitational coupling strength κ_5 of the bulk. In fact let us consider the approximate resonance condition (34), $R(m, E_0, \sigma) = 2/n$. Solving this condition for σ we obtain

$$|\sigma| = \mathcal{F}(m, E_0, 2/n). \tag{35}$$

For fixed $m = 8$ and $E_0 = 0.013$, the function $\mathcal{F}(m, E_0, \mu)$ versus μ is plotted as the continuous line in figure 7. The small circles on the continuous line depict the points corresponding to the discrete values $\mu = 2/n$ associated with the resonances. We then see that the larger the resonance, the stronger the gravitational interaction in the braneworld universe inflated from initial conditions connected with the resonance considered. For the exact dynamics these small circles will extended to n small discrete spots (not shown here) exhibiting a *quantization* of the brane tension and consequently of the gravitational coupling strength in the respective brane inflated due to a specific resonance. An upper bound for σ is also obtained, which will be fixed by m and E_0 and also by the value of the cosmological constant adopted.

Finally a discussion of the structural stability of the above resonance pattern is in order. A careful examination of the basic equations (25), (26) and (34), together with the restriction (28), shows that the ranges of the parameters defining the non-linear resonance domains are fixed basically by the value of Λ adopted (for numerical convenience we adopted in our experiments the value $\Lambda = 1.5$). Indeed the smaller the value of Λ, the larger the height of the barrier in the potential of figure 1(a) implying the existence of bounded solutions for a larger domain of σE_0 and leading to a decrease in values of m corresponding to the dominant resonances. We verify that a decrease of one order of magnitude in Λ results in a decrease of the values of m for the dominant resonances of about the same order of magnitude. For instance if we adopt $\Lambda = 0.1$ we obtain $m \simeq 0.5$

for the resonance $n = 2$ corresponding to a value of $\sigma E_0 = 19.0$. However the underlying pattern of resonance windows and their internal substructure is maintained, being similar to that of the figures shown above in the paper. In this sense the pattern is said to be structurally stable. Once, for instance, the parameters m and Λ are determined, the particular resonance might be fixed as well as the small range of values for E_0 and σ that would allow inflation to occur.

5. Conclusions and final discussion

In this paper we have examined the dynamics of spatially closed inflationary models in which high energy corrections to general relativity are considered, leading to the presence of non-singular bounces in the scale factor of the models. These corrections arise from local bulk effects on the four-dimensional FRW braneworld, in the realm of a Randall–Sundrum-type theory; for the case of a timelike extra dimension the corrections result in a repulsive force that avoids the singularity and provide a concrete model for bounces in the early phase of the universe. The matter content of the model, confined to the FRW brane, consists of a radiation fluid plus a massive scalar field (the inflaton field). The latter enters in the dynamics as small spatially homogeneous expectation values of its fluctuations about the vacuum configuration. Therefore we use the approximation that the local high energy corrections from the bulk, proportional to the square of the energy density, are dominated by the radiation fluid. The resulting dynamics is non-integrable and chaotic if the mass of the inflaton $m \neq 0$, and represents a pre-inflationary phase of the universe with a non-trivial dynamics before the exit to inflation.

We restrict ourselves to dynamical configurations in which the scale factor is initially bounded, bouncing in a potential well arising in the gravitational sector due to the effective cosmological constant, the positive spatial curvature and the high energy corrections from the bulk. They have the theoretical advantage over one-single-bounce models in that they avoid the problem of initial conditions for the universe at past infinity. These metastable configurations are disrupted at later times by non-linear parametric resonances of KAM tori that drive the universe into a inflationary regime.

Non-linear resonance of KAM tori takes place for particular domains of the parameter space (σ, m, E_0) of the model, called windows of resonance, resulting in a complex phase space dynamics. Each resonance is characterized by an integer $n \geq 2$ and its main feature is the bifurcation of the stable periodic orbit at the origin $(\varphi = 0, p_\varphi = 0)$ into an unstable periodic orbit accompanied by one or two characteristic stable periodic orbits according to whether n is odd or even respectively. Since the initial conditions of the expectation values φ are assumed to be small and are then taken near the invariant plane $\varphi = 0$, $p_\varphi = 0$, it follows that the parametric domains of resonance are the ones that allow for inflation in the system. Now if we adhere to the view—strongly sustained by observations—that inflation is a sound paradigm for cosmology, then the values of the parameters of the braneworld model must be constrained to the resonance windows of the parameter space. In particular the brane tension σ, which regulates the relation between the strength of the gravitational coupling in the 5-dim bulk and in the brane, will be restricted to small sheets (depending on the integer $n \geq 2$) as shown in figure 2. In this instance the larger the order of the resonance, the stronger the gravitational interaction in the braneworld universe inflated from initial conditions connected with the resonance considered. For

fixed m and E_0 we observe a *quantization* of the brane tension and consequently of the gravitational coupling strength in the respective brane inflated due to a specific resonance. Also through a careful numerical examination we observe that the pattern of resonance windows in the parameter space of the model is structurally stable, with the range of the parameters defining the non-linear resonance domains being fixed basically by the value of Λ adopted. For a large domain of σE_0 the decrease of Λ leads to a decrease in values m corresponding to the dominant resonances; in particular we verify that a decrease of one order of magnitude in Λ results in a decrease of the values of m for the dominant resonances of about the same order of magnitude. However the underlying pattern of resonance windows and their internal substructure is maintained. In this sense the pattern is said to be structurally stable.

Three distinct dynamical patterns are set up by the resonance, according to the above mentioned substructures in the resonance windows. As illustrated in figure 3, if the initial conditions correspond to configurations in the lower region of the resonance tongue we have short time disruption of the bounded orbit with a rapid escape to inflation. On the other hand, if the initial conditions correspond to configurations in the threshold region of the tongue the orbit undergoes a long time diffusion in the stochastic sea surrounding the main KAM stability islands of the resonance, characteristic of quasi-turbulent regimes, before escape to inflation. Finally for initial conditions connected to the upper part of the tongue the orbit undergoes diffusion without escaping to inflation up to times larger than $\tau = 100\,000$. This latter domain of the resonance window must also be excluded on physical grounds since they correspond to configurations that do not realize inflation.

We should also mention that the number of invariant tori in the case of $n =$ even resonances is twice the number of invariant tori in the case of $n =$ odd resonances, and for an $n =$ even resonance two distinct invariant tori (each about one of the two distinct characteristic periodic orbits of the resonance) may end up with the same energy (they differ by $\varphi \to -\varphi$). However this *degeneracy* in the classical configuration could be raised in a quantum version of the bounded dynamics with possible tunneling between these two classically allowed regions, with the quantum state having a non-null amplitude on both tori. Therefore expected tunnelings enhanced by resonances between the classically allowed regions inside and outside the well of figure 1(a) do not have to be treated separately, in an eventual quantum version of the dynamics.

Finally, if the above processes actually occur in the early dynamics of the universe, the spectrum of perturbations should then have a signature of the particular resonance and consequently of the particular value of the parameters (σ, m, E_0) that were favored in the early dynamical regime of the universe.

Acknowledgments

The authors acknowledge partial financial support from CNPQ/Brazil. Several of the figures were generated using the *Dynamics Solver* package [18]. EVT acknowledges a grant from FUNCEFETES/Brazil.

References

[1] Dienes K R, *String theory and the path to unification: a review of recent developments*, 1997 *Phys. Rep.* **287** 447 [SPIRES]
Kaku M, 2000 *Strings, Conformal Fields and M-theory* (New York: Springer)

Rovelli C, *Loop quantum gravity*, 1998 *Living Rev. Rel.* **1** 1
[2] Randall L and Sundrum R, 1999 *Phys. Rev. Lett.* **83** 4690 [SPIRES]
Randall L and Sundrum R, 1999 *Phys. Rev. Lett.* **83** 3370 [SPIRES]
[3] Shtanov Y V, 2000 *Preprint* hep-th/0005193
Shtanov Y V, 2002 *Phys. Lett.* B **541** 177 [SPIRES]
Shtanov Yu and Sahni V, 2003 *Phys. Lett.* B **557** 1 [SPIRES]
[4] Shiromizu T, Maeda K and Sasaki M, 2000 *Phys. Rev.* D **62** 024012 [SPIRES]
[5] Maartens R, 2000 *Phys. Rev.* D **62** 084023 [SPIRES]
Maartens R, 2004 *Preprint* gr-qc/0312059
[6] Starobinsky A A, 1978 *Sov. Astron. Lett.* **4** 82
[7] Belinsky V A, Grishchuk L P, Zel'dovich Ya B and Khalatnikov I M, 1985 *Sov. Phys. JETP* **62** 195 [SPIRES]
[8] Wald R M, 1984 *General Relativity* (Chicago: University of Chicago Press)
[9] Israel W, 1966 *Nuovo Cim.* **44B** 1 [SPIRES]
[10] Faraoni V, 2000 *Phys. Rev.* D **62** 023504 [SPIRES]
[11] Birrel N D and Davies P C, 1982 *Quantum Fields in Curved Spacetimes* (Cambridge: Cambridge University Press)
[12] Mielke A, Holmes P and O'Reilly O, 1992 *J. Dyn. Differ. Eqns* **4** 95
Hirsch M W, Smale S and Devaney R L, 2004 *Differential Equations, Dynamical Systems & An Introduction to Chaos* (New York: Elsevier Academic Press)
Monerat G A, Oliveira H P and Damião Soares I, 1998 *Phys. Rev.* D **58** 063504 [SPIRES]
[13] Oliveira H P, Damião Soares I and Tonini E V, 2006 *J. Cosmol. Astropart. Phys.* JCAP02(2006)015 [SPIRES]
[14] Abramowitz M and Stegun I, 1964 *Handbook of Mathematical Functions* (*NBS Applied Math. Series* vol 55) (Washington, DC: National Bureau of Standards)
[15] Kolmogorov A N, 1979 *Stochastic Behaviour in Classical and in Quantum Hamiltonian Systems* (*Lecture Notes in Physics* vol 93) ed G Casati and J Ford (Berlin: Springer)
Arnold V I, 1963 *Russ. Math. Surv.* **18** 9
Moser J, 1962 *Nachr. Akad. Wiss. Goett., Math.-Phys. Kl.* IIa **2** 1–20
[16] Guckenheimer J and Holmes P, 1983 *Dynamical Systems and Bifurcations of Vector Fields* (New York: Springer)
[17] Chirikov B V, 1979 *Phys. Rep.* **52** 263 [SPIRES]
[18] Aguirregabiria J M, *Dynamics Solver*, 2006 http://tp.lc.ehu.es/jma.html

JCAP10(2007)008